Enhancement of Absorption Performance Due to the Wavy Film of the Vertical Absorber Tube

Jungkuk Kim, Keumnam Cho*†

Graduate School of Mechanical Engineering, Sungkyunkwan University, Suwon 440-746, Korea

**School of Mechanical Engineering, Sungkyunkwan University, Suwon 440-746, Korea*

Key words: Absorption performance, Vertical absorber, Wavy film flow

ABSTRACT: Absorption performance at the vertical interface between refrigerant vapor and liquid solution of LiBr-H_2O solution was enhanced by the waves formed due to the interfacial shear stress. The present study investigated experimentally and analytically the improvements of absorption performance in a falling film by wavy film flow. The dynamic parameter was the film Reynolds numbers ranged from 50 to 150. The energy and diffusion equations were solved simultaneously to find the temperature and concentration profiles at the interface of liquid solution and refrigerant vapor. Absorption characteristics due to heat and mass transfer were analyzed for the falling film of the LiBr aqueous solution contacted by refrigerant vapor in the absorber. Absorption performance showed a peak value at the solution flow rate of Re_f>100. Absorption performance for the wavy film flow was found to be greater by approximately 10% than that for uniform film flow. Based on numerical and experimental results, the maximum absorption rate was obtained for the wavy flow caused by spring insert. The difference between the measured and the predicted results were ranged from 5.8 to 12%.

Nomenclature

A : surface area [m^2]
C : LiBr-H_2O solution concentration [wt%]
C_p : constant-pressure specific heats [kJ/kg K]
C_s : liquid-vapor interface concentration [wt%]
D : diffusion coefficient [m^2/s]
d : diameter [m]
d_h : hydraulic diameter, $d_a - d_o$ [m]
F : fouling factor [$m^2℃/W$]
G : absorption mass flux [kg/m^2K]
h : heat transfer coefficient [kW/m^2K]
L : length of absorber tube [m]
$LMTD$: log mean temperature difference, $(\Delta T_1 - \Delta T_2)/\ln(\Delta T_1/\Delta T_2)$ [K]
M : absorption rates [kg/s]
$\dot{m}$: mass flow rate [kg/s]
Pr : Prandtl number
P_{ref} : refrigerant vapor pressure [mmHg]
q : heat flux [kW/m^2]
$\dot{Q}$: heat flow rate [kW]
r : coordinate of film thickness [m]
Re_f : film Reynolds number, $4\Gamma_S/\mu_S$
Sh : Sherwood number
T : temperature [K]
U : overall heat transfer coefficient [kW/m^2K]
u : bulk velocity [m/s]
x : coordinate of film flow [m]

† Corresponding author
Tel.: +82-31-290-7445; fax: +82-31-290-7923
E-mail address: keumnamcho@skku.edu

Greek symbols

α : inner tube of coolant channel
β : mass transfer coefficient [m/s]
Γ : mass flow rate per circumferential length [kg/m s]
Δ : film thickness per unit length [m]
δ : local wave altitude [m]
λ : wave length [m]

Subscripts

1 : inlet
2 : outlet
c : coolant
f : film
i : inner tube of absorber
lm : arithmetic mean
o : outer tube of absorber
s : solution
ss : stainless steel
w : surface of absorber tube

1. Introduction

The absorption refrigeration system for residential application has to be air-cooled, compact, and highly efficient system for competing with the vapor compression system. As one of major components affecting the absorption system, an absorber is strongly related with the absorption system performance. Especially, the heat and mass transfer in the vertical absorber affects the performance of the absorption refrigeration system. Literatures on the heat and mass transfer characteristics in the vertical absorber are not completed yet. The design guidelines for the optimal absorber design are mainly dependent on the empirical results with limited experimental operating conditions and the certain systematic parameters. The performance of the absorption system can be improved by enhancing the absorption performance of the absorber. The energy and diffusion equations were solved by Grossman[1] for laminar films on both isothermal and adiabatic walls. As a function of normalized absorber length, charts for calculation of the film's Nusselt and Sherwood numbers were produced. A simple model for the absorption of refrigeration vapor into falling films was described by Andberg and Vliet,[2] based on the pre-assumed similarity of the concentration profiles. Non-isothermal absorption in the wavy laminar films were experimentally characterized in Yueksel and Schluender,[3] and their theoretical predictions were agreed with the measured absorption performance within 30%. Patnaik et al.[4] and Conlisk[5] have developed design tools for absorber with NH_3-H_2O and LiBr-H_2O mixtures into falling films on smooth tubes.

Some experimental studies have been carried out to check the effect of absorber geometry[6] on the absorber performance. Morioka and Kiyota[7] proposed an optimal thickness of the vertical falling film for the maximum absorbing rate of refrigerant vapor. Ohm et al.[8] measured heat and mass transfer coefficients in a vertical copper absorber with the inner diameter of 25 mm for the film Reynolds number from 35 to 150. The absorbing performance in the absorber tube may be affected by both the geometric factors such as tube diameter, length, material and dynamic factors such as solution concentration, solution temperature and pressure, solution flow rate, flow pattern, and etc. The effect of both the flow pattern by the geometric and dynamic parameters on the absorbing performance should be analytically and experimentally investigated.

The present study investigated the effect of the falling film flow pattern due to the geometric difference on the absorption performance in a vertical falling-film absorber using LiBr-H_2O solution with 60 wt%.

2. Model and equation

A schematic diagram of the falling-film wavy flow on the vertical-tube absorber is shown in

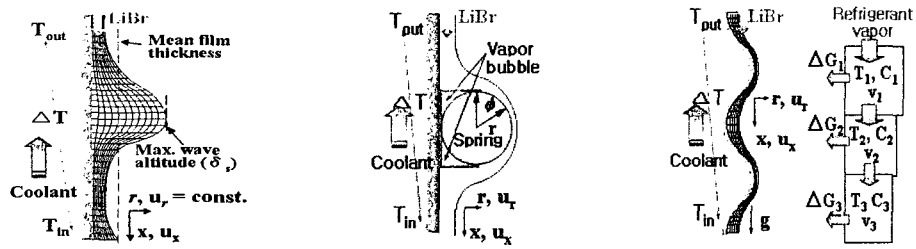

(a) Bare & grooved tube (b) Tube with spring insert (c) Corrugated tube

Fig. 1 *Analytical model of a vertical absorber.*

Fig. 1. The coolant and LiBr solution flow counter-currently while the absorption heat is wholly transferred to the coolant. The solution flows as a falling film in the inner surface of the absorber tube, entering concentrated at the top and leaving diluted at the bottom of the tube after absorbing refrigerant vapor. Numerical solution of the governing equation for the coupled heat and mass transfer problem yields the temperature and solution concentration profiles, based on the following assumptions.

The system is at the steady-state and considered as a two-dimensional problem. The specific heats of both coolant and LiBr solution are nearly constant, and the heat transfer coefficient on the coolant side of the absorber is constant. The falling film is laminar flow. The vapor-side resistance to mass transfer and the vapor drag on the falling film are negligible. The vapor mass absorbed is very small compared to LiBr solution flow.

The theoretical model is constructed from the energy and mass balance on the surface of the solution and refrigerant vapor. Under the above-mentioned assumptions, the simultaneous heat and mass transfer at steady-state is described by the energy and diffusion equations.

$$u\frac{\partial C}{\partial x}=D\left(\frac{\partial^2 C}{\partial x^2}+\frac{1}{r}\frac{\partial C}{\partial r}+\frac{\partial^2 C}{\partial r^2}\right) \tag{1}$$

$$u\frac{\partial T}{\partial x}=\left(\alpha\frac{\partial^2 T}{\partial x^2}+\frac{1}{r}\frac{\partial T}{\partial r}+\frac{\partial^2 T}{\partial r^2}\right)+\frac{D\Delta c_p}{c_p}\left(\frac{\partial T}{\partial r}\frac{\partial C}{\partial r}+\frac{T}{r}\frac{\partial C}{\partial r}+T\frac{\partial^2 C}{\partial r^2}\right) \tag{2}$$

where u is the bulk velocity in the x-direction in the liquid and refrigerant vapor phases. The bulk velocity profile is parabolic and given by

$$u=\frac{3}{2}\bar{u}\left\{2\left(\frac{r}{\Delta x}\right)-\left(\frac{r}{\Delta x}\right)^2\right\} \tag{3}$$

where $\bar{u}$ is the average flow velocity, equal to the mass flow rate per length, divided by the density and film thickness.

For two-dimensional laminar flow, the unsteady Navier-Stokes equations for wavy film flow in the coordinate system shown in Fig. 1 are;

$$\frac{\partial u}{\partial t}+u\frac{\partial u}{\partial x}+v\frac{\partial u}{\partial r}=-\frac{1}{\rho}\frac{\partial p}{\partial x}+g+v\left(\frac{\partial^2 u}{\partial x^2}+\frac{\partial^2 u}{\partial r^2}\right) \tag{4}$$

$$\frac{\partial u}{\partial t}+u\frac{\partial u}{\partial x}+v\frac{\partial u}{\partial r}=-\frac{1}{\rho}\frac{\partial p}{\partial x}+v\left(\frac{\partial^2 u}{\partial x^2}+\frac{\partial^2 u}{\partial r^2}\right) \tag{5}$$

The following boundary condition apply

$$C=C_0,\quad T=T_0 \quad \text{at} \quad x=0 \tag{6a}$$

$$\frac{\partial T}{\partial r}=0,\quad \frac{\partial C}{\partial r}=0 \quad \text{at} \quad r=0 \tag{6b}$$

$$r=r_1;\quad C=f(T,P)\qquad \dot{q}_s=k\left(\frac{\partial T}{\partial r}\right)-\Delta c_p T\rho D\left(\frac{\partial C}{\partial r}\right) \tag{7}$$

where Δc_p is difference of specific heat between solution and coolant at the wall.

3. Experimental apparatus and conditions

Figure 2 shows a schematic diagram of the present experimental setup, which consists of an absorber, a generator, a solution tank, an evaporator/condenser, a constant temperature bath, a mass flow meter and a sampling device.

The absorber consisted of an upper header, an absorbing tube and a lower header. The absorber tubes with thickness of 1.0 mm were made of stainless steel tube (SUS316). The LiBr-H_2O solution moved downward in parallel to the gravity from the upper header to the absorbing tube. Then, the weak solution made after absorption process moves toward the lower header of the absorber and then to the solution tank. Thermocouples were installed at the upper and lower headers to measure the temperatures of solutions. The coolant temperatures were also measured at the inlet and outlet of the coolant channel. The pressures at the inlet and outlet of the absorber were measured by an absolute pressure gauge. The strong solution in the generator and weak solution at the outlet of the absorber were extracted by using a sampling trap. The specific gravity was measured by a volumetric flask of 25 ml and an electronic balance with the accuracy of ±0.1 mg. The magnetic solution pump with a capacity of 0.033 kg/s was used to circulate the solution into the absorber.

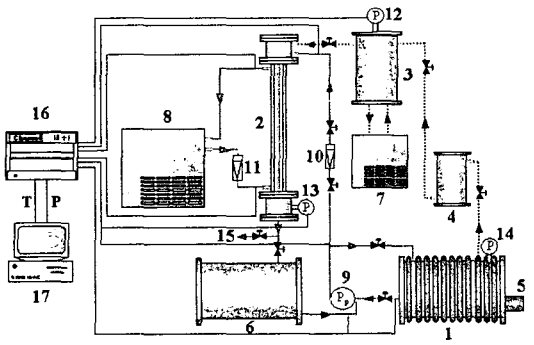

1. Generator
2. Absorber
3. Evaporator
4. Condenser
5. Heater
6. Weak solution tank
7-8. Constant temp. bath
9. Magnetic pump
10-11. Rotameter
12-14. Vacuum pressure gage
15. Sampling trap
16. Data acquisition board
17. PC

Fig. 2 Schematic diagram of the present experimental apparatus.

The geometric parameter was the absorber tube (bare, grooved, spring). The dynamic parameter was the film Reynolds numbers from 50 to 150. The pressure in the absorber was set at 1.01 kPa, and the flow rate of the cooling water was fixed at 0.025 kg/s.

Figure 3 (a) shows the film flow pattern by the shape of absorber. Film separation and instability flow in the bare tube were increased as the wall roughness was increased. But the micro-grooved tube and tube with spring in Fig. 3 (b) and (c) show the uniform film due to the increase of the frictional force between LiBr solution and absorber wall.

(a) Bare tube (b) Grooved tube (c) Spring tube

Fig. 3 Photographs of flow pattern (Re_f=90).

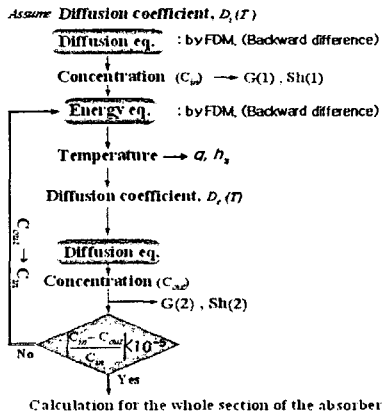

Fig. 4 Flow chart of the numerical analysis.

The flow chart for calculating absorption rate of the absorber tube is shown in Fig. 4.

4. Data reduction

4.1 Heat transfer

The heat transfer rate from the solution to the coolant is obtained by the Eq. (8).

$$\begin{aligned} \dot{Q} &= \dot{m}_c C_{p.c}(T_{c.2} - T_{c.1}) \\ &= U_s A_s LMTD \end{aligned} \tag{8}$$

The heat flux (q) is obtained by dividing the heat transfer rate in the Eq. (8) by the heat transfer area. The overall heat transfer coefficient is obtained by the Eq. (9).

$$U_S = \frac{1}{\frac{A_i}{A_o}\frac{1}{h_c} + \frac{A_i \ln\left(\frac{r_o}{r_i}\right)}{2\pi k_{ss} L} + \frac{1}{h_s} + F} \tag{9}$$

The fouling factor (F) which can be applied for an absorption system is 0.00015 m^2℃/W. r_o and r_i are the inlet and outlet radius of absorber. The convective heat transfer coefficient, h_c, can be determined by the following Eq. (10) suggested by the literature (9), which can be applied for laminar flow in vertical tube.

$$\mathrm{Nu}_c = \left[\mathrm{Nu}_\infty + f \frac{0.19\left(\mathrm{Re}_c \mathrm{Pr}_c \frac{d_h}{L}\right)^{0.8}}{1 + 0.117\left(\mathrm{Re}_c \mathrm{Pr}_c \frac{d_h}{L}\right)^{0.467}} \right] \times \left(\frac{\mathrm{Pr}_c}{\mathrm{Pr}_w}\right)^{0.11} = \frac{h_c d_h}{k_c} \tag{10}$$

The heat transfer coefficient in an absorber can be obtained by using Eqs. (8) to (10).

According to the uncertainty analysis suggested by Moffat[10] as shown in Eqs. (11), the heat transfer coefficient have the error from ±1.2 to ±3.1%.

$$\frac{\delta h_s}{h_s} = \sqrt{\left[\frac{\delta(\dot{Q})}{\dot{Q}}\right]^2 + \left[\frac{\delta(A)}{A}\right]^2 + \left[\frac{\delta(T_{s,1})}{\Delta T_{lm}}\right]^2 + \left[\frac{\delta(T_{s,2})}{\Delta T_{lm}}\right]^2} \tag{11}$$

4.2 Mass transfer

The absorption rate is shown by

$$M = GA_i = \dot{m}_s\left(\frac{C_{s,1}}{C_{s,2}} - 1\right) \tag{12}$$

The mass transfer at a falling film occurred by the difference between the solution concentration at the liquid-vapor interface and average concentration of a falling film. Since the solution concentration at liquid-vapor interface cannot be measured, it can be replaced with the saturated concentration at the pressure in the absorber and the solution temperature. The absorption rate of refrigerant vapor is given by Eqs. (13a) to (13b).

$$M = \rho_s \beta A_i \Delta C_{lm} \tag{13a}$$

$$\Delta C_{lm} = \frac{(C_{s1} - C_1^s) - (C_{s2} - C_2^s)}{\ln\left[(C_{s1} - C_1^s)/(C_{s2} - C_2^s)\right]} \tag{13b}$$

The mass transfer coefficient can be calculated from Eqs. (12) and (13). The Sherwood number can be obtained by Eq. (14).

$$\mathrm{Sh} = \frac{\beta L_s}{D_s} \tag{14}$$

According to the uncertainty analysis suggested by Moffat[10] as shown in Eqs. (15), the absorption rate showed the error range from ±2.7 to ±4.3%.

$$\frac{\delta M}{M} = \sqrt{\left[\frac{\delta(\rho_s)}{\rho_s}\right]^2 + \left[\frac{\delta(\beta)}{\beta}\right]^2 + \left[\frac{\delta(A_s)}{\Delta A}\right]^2 + \left[\frac{\delta(C_{s,1})}{\Delta C_{lm}}\right]^2 + \left[\frac{\delta(C_{s,2})}{\Delta C_{lm}}\right]^2} \tag{15}$$

5. Results and discussion

5.1 Effect of wave length

Figure 5 shows maximum wave altitude and critical maximum film thickness with respect to the wave length in the numerical analysis. The maximum wave altitude for $\lambda<0.02$ m was decreased rapidly at constant concentration and temperature of LiBr solution. The maximum wave altitude for $\lambda>0.02$ m was predicted as 0.319 mm due to the increase of the frictional force between LiBr-solution and absorber wall.

The maximum wavy film thicknesses of periodic wave for $\lambda>0.02$ m was higher by 2.2~3.0% than those of mean film thickness of uniform film. It was also found that the effect of the wave length on the wave altitude showed a similar trend.

5.2 Heat transfer

The present study has been done under the following: $C_{s,1}=60$ wt%, $T_{s,1}=45$℃, $T_{c,1}=30$ ℃, $P_{ref}=7.6$ mmHg and $Re_f=30\sim160$.

Figure 6 shows the Nusselt numbers with respect to the wavy film flow pattern at the film Reynolds numbers from 30 to 160.

The heat transfer coefficients were small at a low film Reynolds number due to the non-uniform and unstable film formed in the absorber. The heat transfer coefficients were increased and then kept almost constant over the film Reynolds number of 90 due to the stable liquid formed at the Reynolds number.

Measured heat fluxes were increased by the maximum of 30% as wavy film flow pattern (uniform flow, wavy flow, rapidly wavy flow in tube with spring) changed. The analytical results were larger by 12.5~25% than measured data due to the assumption taken in numerical analysis. The Nusselt numbers were decreased due to the decrease of the local heat transfer area due to the instability of film flow and the increase of local thermal resistance. As the film Reynolds number increased, the film shape became uniform and stable, and the absorption resistance of refrigeration vapor due to the instability of film flow was decreased. The mass transfer rate was increased due to the increase of heat transfer area and absorbing area.

The total heat transfer rate was increased by the sensible heat as the mass transfer rate was increased. The Nusselt number was large in the reverse order of uniform film, wavy film and rapidly wavy flow in tube with spring due to the difference change of surface shape in the absorber.

The Nusselt numbers solved by Grossman[1] were higher than those by the present study at the $Re_f<90$ due to the assumptions of uniform film and constant temperature of wall.

The part of falling film of the solution was

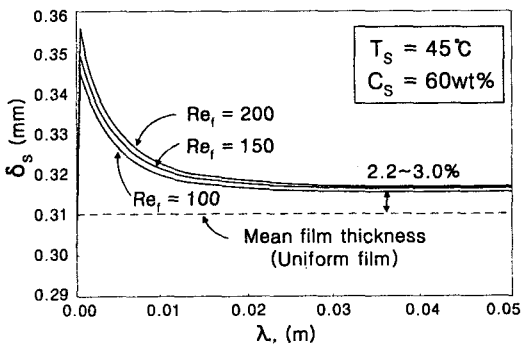

Fig. 5 Effect of λ on maximum wave altitude.

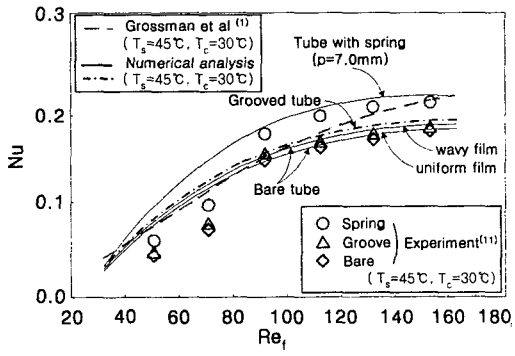

Fig. 6 Effect of wavy film flow pattern on h_s.

separated due to the roughness of wall surface. As the heat transfer area decreased and the thermal resistance by local wettability of absorber increased, the Nusselt number decreased.

5.3 Mass transfer

Figure 7 shows the change of Sherwood number with respect to the Reynolds numbers for wavy film flow pattern in the absorber.

The Sherwood number was significantly increased up to the film Reynolds number of 90, peaked on it, and then slightly decreased. The absorption mass flux as with respect to that of wavy film flow pattern were large distinct over the film Reynolds number of 90 than those below that.

As the wavy film changed for uniform flow to the rapidly wavy flow in tube with spring, the Sherwood number at tube with spring were increased by the maximum of 25%. Numerical results by Grossman[1] were higher by the maximum of 16.6% than those by the present study at $Re_f>90$. The differences from the data by Grossman[1] were caused due to the assumption (constant temperature of wall, constant diffusion coefficient), flow pattern (uniform film flow). Those assumption led to the increase of absorption performance compared with the present study.

The diffusion coefficient at the outlet of absorber was decreased by the absorption of refrigerant vapor in the absorber, and the temperature of wall of absorber increased by the heat flux between LiBr-solution and coolant in the practical case.

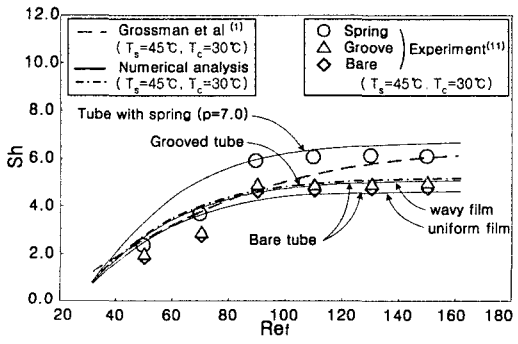

Fig. 7 Effect of wavy film flow pattern on *G*.

The constant diffusion coefficient of the solution induced more absorption rates and the constant temperature of coolant caused the increase of the absorption rates. The numerical result was larger by 5~15% than the experimental result. The difference between numerical and experimental result was from the same reason with the effect of flow instability and increase of local thermal resistance by local wettability during the heat trasnfer process.

6. Conclusions

(1) The maximum wave altitude of periodic wave for $\lambda>0.02$ m was higher by 2.2~3.0% than that of uniform film with mean film thickness, and the effect of wave length on the wave altitude showed a similar trend.

(2) As film wavy flow by the surface shape increased, the absorption mass flux and heat transfer coefficient increased from uniform flow < wavy flow < rapidly wavy flow in tube with spring.

(3) The absorption performance was affected by the mass flow rate rather than the flow pattern.

(4) As the instability of film flow increased, the numerical values were getting higher than the measured data. The difference ranged from 5.8 to 12%.

Acknowledgement

This work was supported by the Brain Korea 21 project.

References

1. Grossman, G., 1983, Simultaneous heat and mass transfer in film absorption under lami-

nar flow, Int. J. Heat and Mass Transfer, Vol. 26, No. 3, pp. 357-371.
2. Andberg, J. W. and Vliet, G. C., 1983, Design guidelines for water-lithium bromide absorbers, ASHRAE Transactions, Vol. 89, No. 1B, pp. 220-232.
3. Yueksel, I. and Schluender, W., 1988, A model of an ammonia-water falling film absorber, ASHRAE Transactions, Vol. 94, No. 1, pp. 467-483.
4. Patnaik, V., Perez-Blanco, H. and Miller, W. A., 1992, Experimental validation of a simple analytical model for the design of vertical tube absorbers, In progress.
5. Conlisk, A. T., 1995, Analytical solution for the heat and mass transfer in a falling film absorber, Chemical Engineering Science, Vol. 50, No. 4, pp. 651-660.
6. Yoon, J. I., Oh, H. K. and Takao, K., 1995, Characteristics of heat and mass transfer for a falling film type absorber with insert spring tubes, Transaction of KSME, Vol. 19, No. 6, pp. 1501-1509.
7. Morioka, I. and Kiyota, M., 1987, Absorption of water vapor into a lithium-bromide water solution film falling along a vertical plate, Transactions of the JSME (Part B), Vol. 53, No. 485, pp. 236-240.
8. Ohm, K. C., Kashiwagi, T. and Seo, J. Y., 1993, Characteristics of absorption and heat transfer for film falling along a vertical inner tube (Characteristics of absorption), Korean Journal of Air-Conditioning and Refrigeration Engineering, Vol. 5, No. 1, pp. 1-9.
9. Kim, K. J., Berman, N. S. and Wood, B. D., 1995, Absorption of water vapor into falling films of aqueous lithium bromide, Int. J. Refrigeration, Vol. 18, No. 7, pp. 486-494.
10. Moffat, R. J., 1985, Using uncertainty analysis in the planning of an experiment, Trans. of the ASME: J. Of Fluid Engineering, Vol. 107, pp. 173-182.
11. Kim, J. K. and Cho, K. N., 2002. Influence of spring on the absorption performance of a vertical absorber tube, Transaction of SAREK (in Korean), Vol. 14, No. 10, pp. 825-832.